ingegneria sismica
International Journal of Earthquake Engineering
Anno XLIII - Num. 2 - 2026

# Particle swarm algorithm-based user regulation and station autonomy strategies in low-voltage distributed photovoltaic systems

*Guocheng Li*[1], *Cong Wang*[1], *Zeguang Lu*[1], *Ze Zhang*[1,*], *Xiaoran Li*[1] *and Xiaoqin Wang*[1]

[1] State Grid Dezhou Power Supply Company, Dezhou, Shandong, 253000, China

**SUMMARY:** *In the face of the problems of voltage overstepping the limit and three-phase unbalance which are caused by large-scale access of distributed photovoltaic power into low-voltage distribution networks, this research, in a creative way, uses the chaotic particle swarm optimization algorithm. This present application seeks to achieve a result that brings benefits to both sides, hence guaranteeing both the safe and money-saving running of the electric network and the promotion of the benefits of users.On the electric grid part, there exists a coordinating arrangement of energy storage systems, static var generators (SVG), and flexible load resources. At the same time, on the side of users, a model which puts emphasis on economic optimization has been established.Furthermore, through the usage of the chaotic particle swarm optimization (CPSO) algorithm, chaotic sequences are brought into the iterative procedure for enhancing the whole optimization ability. Carry out the development of a cooperative control strategy for three-layer optical storage, that is, storage, reactive power, and active power. Take the intelligent convergence terminal as the central node, carry out real-time monitoring on the condition of the station. First, we ought to give the first place to the use of energy storage for providing fast voltage support. When the storage capacity is not enough, we ought to trigger the reactive power adjustment function that the PV inverter has. Only when the situation is absolutely necessary, we should consider carrying out the reduction of a part of the PV active power. Through this kind of doing, it can be achieved that the station area carries out the self-governance.Compared with the no-optimization state, the strategy in this paper reduces the voltage mean offset (SVA) from 6.36 × 10-3 to 2.66 × 10-3. Before we carry out optimization work, the passing percentage of node voltage inside the station region has been increased from 65.17% to the complete 100%. At the same time, the peak voltage has been lowered from 1.063 per-unit to 1.029 per-unit.*

***KEYWORDS:*** *low voltage distribution network; distributed photovoltaic; chaotic particle swarm algorithm; user regulation; station autonomy*

# 1 Introduction

Under the situation of the rising whole world energy shortage and the progress of the all-round reform inside the energy transformation, traditional fossil fuels such as coal and oil are step by step replaced by renewable energy types, which contain solar energy, wind power, and tide energy. Therefore, a newly appeared energy frame which takes clean energy as core is getting more and more attention from experts and scholars [1-3]. The wide deployment of distributed photovoltaic electricity producing, electric automobiles, clean warming systems, domestic energy storage equipment, and so forth, makes the load of the distribution network to develop

*zhangzedq0801@163.com
https://doi.org/10.65102/is2026595
Published: 30 April, 2026

in the direction of diversification. This development gives both new chances and difficulties to the running and controlling of the distribution network [4, 5]. In the face of the major changes in the source and load ends, the function and form of the distribution network also need to undergo profound changes. Compared with traditional power generation methods, distributed photovoltaic power generation has the advantages of low investment cost, short construction period and no environmental pollution [6, 7]. In the recent several years, distributed photovoltaic (PV) systems have obtained very obvious development, therefore this is promoted by the carry out of new energy policies.

The progress of photovoltaic technique has given a large amount of convenience to we people. But, at the same time, it also brings very many bad influences to the distribution network. The wide employment of distributed photovoltaic power has many kinds of influences upon the power quality of the distribution grid. The incorporation of distributed photovoltaic power systems into the electric grid has changed the original voltage distribution that is inside the distribution network. Fluctuations which are in the output power of these systems bring about varying degrees of reduction in the current that is supplied by the power source. At the same time, they bring about a rising of the voltage on every node of the power distribution network [8-10]. Due to the instability of photovoltaic power generation, changes in external factors such as weather, temperature, air quality, etc., can lead to the instability of PV output power, which leads to fluctuations in grid voltage, affecting the quality of power consumption by users [11, 12]. In addition, with the increase of distributed PV power generation systems, it not only makes the distribution network voltage overrun, but also increases the difficulty of regulation of the distribution network [13].Therefore, thus, it is a necessity that voltage coordination control tactics be formulated by us to make fine adjustments to voltage distribution and hence enhance the stability degree of low-voltage distribution network systems.

Ciocia et al [14] controlled the voltage of a low voltage grid with distributed PV converters, static reactive power compensators and load regulators, which stabilize the voltage at the grid connection point without any coordination between these control devices. Ku et al [15] replaced the reactive power compensator with a PV smart inverter for autonomous control and coordinated the transformer on-load tap-changer for voltage control of distribution feeders, and the practice confirmed that this coordinated control strategy effectively improved the quality of distribution network power supply for PV penetration. However, the static reactive power compensator is difficult to cope with the voltage dynamic regulation demand, while the transformer on-load tap-changer regulation accuracy is insufficient, and the two can not satisfy the coordination of multiple PV inverters on the station area.Furthermore, some research workers regard the voltage adjustment of the low-voltage (LV) distribution network as a multi-goal optimization problem in order to obtain a more superior solution.Spertino et al [16] used simulation experiments to determine the optimal settings of voltage control devices in a low-voltage grid under independent operation of the on-load tap-changer and distributed PV inverters to reduce the voltage deviation at the grid connection point by performing multi-objective optimal solutions with Pareto analysis and approximation to the ideal solution ordering method. However, the simulated voltage control strategy is inefficient and has a slow response in the rapid fluctuation scenario of PV power generation. Therefore, researchers have introduced intelligent optimization algorithms such as evolutionary algorithms, genetic algorithms, and particle swarm algorithms (PSO) into voltage control tasks. Zhang et al [17] represented the distribution network in the distributed photovoltaic system as multiple clusters, exchanging voltage information between the clusters through virtual free nodes, cutting the active power under the condition of compensating the reactive power, and introducing the improved differential evolutionary algorithm for the voltage control, which is a control strategy, which is able to maximize the use of the capacity of the distributed power equipment under the

voltage qualification criterion. Ajayi et al [18] used genetic algorithm to optimize the layout of distributed generation and improved the voltage profile of distributed generation system to guarantee voltage stability, which helps to reduce losses and optimize the efficiency of energy economy operation. In the distribution network adjustment of distributed PV systems, PSO has the advantages of faster convergence, fewer parameters, and simple implementation compared to other intelligent optimization algorithms, which have difficulty in balancing the global search and local optimization problems.

Granule Group Collected Optimization (GCO) is one optimize calculation method that it depends on group wisdom. This method tries hard to find the most superior solution through the imitating of the food searching behavior that a group of birds has. The core of research and promotion work for this algorithm is to raise the convergence speed and the precision of results when handling complex optimization questions. Wang et al [19] proposed an autonomous optimization control strategy for distributed PV based on voltage optimization principle, genetic algorithm and PSO algorithm, which reduces the degree of voltage fluctuation and voltage deviation of distributed PV system and also improves the photovoltaic conversion efficiency ratio. Liu et al [20] constructed a reactive power optimization model, introduced a multi-objective PSO algorithm with adaptive grid and roulette wheel mechanism to obtain the optimal solution for the stochastic fluctuation of distributed PV power supply, and proposed a reactive power control strategy to solve the problems such as voltage overrun and network loss. Kewen et al [21] constructed a multi-objective optimization mathematical model and used an improved multi-objective PSO algorithm to achieve more objective voltage regulation of the PV grid-connected grid to ensure that the network losses, voltage deviations, and operating costs are minimized. Santos et al [22] searched for the optimal power factor of the interface inverter through an improved PSO algorithm to avoid voltage overruns, improve the voltage distribution of the system, and maximize the PV carrying capacity of the LV distribution system. Ping et al [23] created an integrated low and medium voltage control model, designed voltage deviation and network losses as objective functions, optimized active-reactive power coordination, presented as a single objective function through the weight coefficient method, and introduced an improved PSO algorithm to solve the function to achieve integrated low and medium voltage distribution network voltage control. Guan et al [24] proposed an active distribution network voltage regulation control strategy based on an improved PSO algorithm to optimize reactive power and voltage as a control tool to ensure voltage stability in the context of integration of distributed PV systems. Weng et al [25] realized the coordinated control of multiple operation modes in distributed PV systems and maintained the stability of distribution network operation by establishing a mathematical model of the inverter main controller and introducing an adaptive variational PSO algorithm solution with a larger search range.

In addition, the PSO algorithm helps to meet the distributed PV power distribution grid operation needs and area control requirements. Liu et al [26] used PSO and binary PSO algorithms to solve a two-tier coordinated siting and sizing planning model for optimal layout and sizing of distributed PV energy storage devices in distribution grids to avoid under-distribution of currents and voltages in grid operation. The standard PSO is prone to lead to local optimization in high-dimensional and complex adjustment scenarios, and most of the studies do not focus on coordination under multiple time scales, resulting in insufficient minute-level response for station autonomy.

The study starts from the starting point, through the storage PV cooperative control strategy, to realize the station autonomy and user regulation, taking into account the user's economy and power experience. First of all, a cooperative optimization model which is for the power grid side as well as the consumer side has been established. Upon the electric power network side, the principal objective is to reduce network energy losses. For reaching this target, the

regulation abilities of energy storage systems, reactive power equipment, and flexible loads are put together to be combined. By comparison, the consumer aspect has the goal to cut down the cost that electric power use brings and make the obtained benefits from this reach the maximum. This stimulation pushes consumers to actively take part in demand-side reaction. The two models are coupled together by power balance, voltage and current constraints, and energy storage state to achieve multi-layer collaborative optimization. For solving the problem of nonlinear solutions that exist inside the model, a kind of chaotic particle swarm optimization algorithm is put forward. This algorithm is constructed on the basis of the traditional particle swarm through the integration of the traversal characteristics of chaotic sequences. Therefore, it can effectively carry out the prevention of early convergence, promote the ability of global optimization, and is very suitable for solving the problem of grid scheduling that includes very many variables and complex constraint conditions.For the enhancement of the active self-governance of the station area, a cooperative control strategy of optical storage is hence devised. This tactic puts the intelligent convergence terminal at the core, which is used as a central spot for real-time monitoring of the operation condition of the station area. After the over-voltage condition has been found out, the energy storage system is given the first priority to carry out fast adjustment. When the situation appears that energy storage storage capacity has not sufficient amount, the function that provides reactive power support of PV inverter is been started. If the requirements are still not achieved, a moderate cut of PV active power is considered by us for releasing reactive capacity. In the whole of this process, the chaotic particle swarm algorithm is utilized by us to carry out the optimization of parameters.

# 2 Optical storage cooperative optimization model and station autonomy strategy based on chaotic particle swarm algorithm

## 2.1 Energy regulation model for low voltage distribution networks

In the present research treatise, a three-phase four-wire system is utilized by the researchers to build the network topology of the low-voltage distribution network that is based on the nodal conductance matrix. For the purpose that the economic running of the network can get optimization, a multi-time period cooperative optimization controlling model is established by us. This model inside has the active strength of energy storage tools, the reactive strength of energy storage tools, the reactive strength of Static Var Generators (SVG), and flexible load devices. Furthermore, this research has already taken into consideration the constraint problems which are related to the three-phase imbalance degree, voltage, and current.

### 2.1.1 Grid-side optimization model

(1) Objective function

For realizing the target of cutting network loss quantities, an optimized current model for the distribution network which is established on the basis of a three-phase four-wire system is constructed. The factors needing optimization are the active and reactive energy storage at the power grid side, the SVG reactive power magnitude, and the adjustable active power at the user side.

$$\min F = \sum_{t=1}^{T} P_t^{loss} \Delta t \tag{1}$$

$$P_t^{loss} = \left[ I_t^{line*} \otimes I_t^{line} \right]^T R^{line} \tag{2}$$

(2) Constraints

1) Voltage constraints

In order to guarantee the power grid can carry out its work in a secure and stable way, the voltage size on each node of the distribution network must work inside the stipulated scope.

2) Neutral line voltage constraint

For guarantee that the line can do its work in secure and steady way, the voltage scope of the neutral line must locate inside the biggest allowed limits.

3) Current constraint

For guarantee the secure and stable work of the line, the current inside the branch circuit must be held within the safe scope.

4) Three-phase unbalance constraints

The non-balance of three-phase system is an important measuring index for the safe and stable movement of the three-phase four-wire system electric network. This measurement is carried out by the ratio which the voltage's negative sequence component has to its positive sequence component.

$$U_{m,t}^{VUF} = \frac{\left| V_{m,t}^{neg} \right|}{\left| V_{m,t}^{pos} \right|} = \frac{\left| V_{m,t}^{a} + \alpha^2 V_{m,t}^{b} + \alpha V_{m,t}^{c} \right|}{\left| V_{m,t}^{a} + \alpha V_{m,t}^{b} + \alpha^2 V_{m,t}^{c} \right|} \tag{3}$$

$$U_{m,t}^{VUF} \le U_{\max}^{VUF} \tag{4}$$

where: $V_{m,t}^{neg}$ and $V_{m,t}^{pos}$ are the negative-sequence and positive-sequence voltages on phases $a$, $b$, and $c$ of bus $m$, respectively; $V_{m,t}^{a}$, $V_{m,t}^{b}$, and $V_{m,t}^{c}$ are the voltages corresponding to the $a$, $b$, and $c$ phases on bus $m$, respectively; $\alpha$ is 120 degrees; $U_{\max}^{VUF}$ is the maximum value of three-phase unbalance allowed.

The maximum voltage deviation index (MVDI) can be utilized by people to measure the voltage deviation that is inside the network. We give its definition in the following way:

$$V_{dev} = \max \frac{\left| V_i - V_{ref} \right|}{V_{ref}} \times 100\% \ \forall i \in N \tag{5}$$

where: $V_{ref}$ is the reference voltage of the node.

5) Energy storage constraints

When we consider the incorporation of a large amount of distributed photovoltaic (PV) systems into the electric power grid, the distribution grid is equipped with adjustable energy storage devices which are constrained by state - of - charge (SOC) restrictions.

$$S_{\min}^{soc} \le S_{i,t}^{soc} \le S_{\max}^{soc} \tag{6}$$

6) Incremental benefit constraint

In this research paper, the decrease of network losses which is caused by user participation in user-side adjustment is regarded as the extra income for network operation. Through utilizing the cost reductions obtained via user joining in user-side adjustment to be a stimulation for users,

this circumstance can be depicted in the following way:

$$I_{net} = (Q_c + \mu_c K_c)\Delta W^{loss} \tag{7}$$

$$\Delta W^{loss} = \sum_{t=1}^{T} \left[ P_{before,t}^{loss} - P_{after,t}^{loss} \right] \Delta t \tag{8}$$

where: $I_{net}$ is the incremental benefit of network operation; $Q_c$ is the cost of generating a unit of kWh; $\mu_c$ is the price of the carbon tax; $K_c$ is the amount of $CO_2$ produced per unit of kWh generated from a conventional coal-fired plant, and $\Delta W^{loss}$ is the amount of change in network losses; $P_{before,t}^{loss}$ is the grid loss before user regulation; $P_{after,t}^{loss}$ is the grid loss after user regulation.

(3) Establishment of convex optimization model

The grid-side optimization model is convexized to transform the non-convex nonlinear problem of the original optimization model into a convex planning problem that is easy to solve.

1) Complex splitting

Split all complex variables into two parts, real and imaginary.

$$V_t = V_t^{real} + jV_t^{imag} = \left(\mathrm{Re}(Y) + \mathrm{Im}(Y)\right)^{-1} \left(I_t^{inj,real} + jI_t^{inj,imag}\right) \tag{9}$$

The superscripts *real* and *imag* are the real and imaginary parts of the variables, respectively; $V_t^{real}$ is the real part of the vector of voltage values at each node; $I_t^{inj,real}$ is the real part of the vector of current values injected at each node; $I_t^{inj,imag}$ is the imaginary part of the vector of injected current values at each node; $\mathrm{Re}(\cdot)$ and $\mathrm{Im}(\cdot)$ are the real and imaginary parts of the matrix. The real and imaginary parts of the voltage at each node are denoted as:

$$V_t^{real} = \left(\mathrm{Re}(Y)\right)^{-1} I_t^{inj,real} - \left(\mathrm{Im}(Y)\right)^{-1} I_t^{inj,imag} \tag{10}$$

$$V_t^{real} = \left(\mathrm{Im}(Y)\right)^{-1} I_t^{inj,real} - \left(\mathrm{Re}(Y)\right)^{-1} I_t^{inj,imag} \tag{11}$$

2) Voltage Upper Limit Constraint

The essence of the voltage upper bound constraint is that the modulus of its complex is less than the voltage upper bound value, i.e.:

$$\left(v_{i,t}^{real}\right)^2 + \left(v_{i,t}^{imag}\right)^2 \le \left(V_i^{\max}\right)^2 \tag{12}$$

3) Voltage lower limit constraint

The restriction of the lower voltage boundary is, it should be pointed out, a concave function, thus it is hard to search for the optimal value. For getting the most excellent solving result, this paper carries out linear processing on the constraint, the concrete content is as follows:

$$-k_{1a} v_{i,t}^{a,real} - k_{2a} v_{i,t}^{a,imag} \le -V_i^{\min} \tag{13}$$

$$-k_{1b}v_{i,t}^{b,real}-k_{2b}v_{i,t}^{b,imag}\le -V_i^{\min} \tag{14}$$

$$-k_{1c}v_{i,t}^{c,real}-k_{2c}v_{i,t}^{c,imag}\le -V_i^{\min} \tag{15}$$

where: $k_{1a}$ and $k_{2a}$ are the lower pressure limit constraint coefficients for the $a$ phase, with values of 1.002 and 0, respectively; $k_{1b}$ and $k_{2b}$ are the lower pressure limit constraint coefficients for the $b$ phase, with values of -0.5003 and - 0.8665; $k_{1c}$ and $k_{2c}$ are the lower pressure limit constraint coefficients for the $c$ phase with values of -0.5003 and 0.8665, respectively.

4) Three-phase unbalance constraint

According to the equation that describes three-phase unbalance, it is very clear that both the expression of negative-sequence voltage which is in the numerator and the expression of positive-sequence voltage which is in the denominator are convex functions. However, when it is subjected to the three-phase unbalance constraint, the ratio of these two just forms a concave function. In addition, in the actual world three-phase four-wire power distribution network, the numerical value of the negative-sequence voltage on each node is obviously lower than that of the positive-sequence voltage, and its mode length is approximately equal to the voltage magnitude of the node, so the three-phase unbalance degree equation can be approximated as:

$$U_{m,t}^{VUF}=\frac{\left|V_{m,t}^{neg}\right|}{\left|V_{m,t}^{pos}\right|}\cong\frac{\left|V_{m,t}^{a}+\alpha^2V_{m,t}^{b}+\alpha V_{m,t}^{c}\right|}{V_{\varphi,t}} \tag{16}$$

$V_{\varphi,t}$ is the rated voltage value of $\varphi$.

5) Neutral line voltage constraint

Split the neutral line voltage into two parts, real and imaginary:

$$\left(V_{i,t}^{real}\right)^2+\left(V_{i,t}^{imag}\right)^2\le\left(V_{neut}^{\max}\right)^2 \tag{17}$$

$V_{neut}^{\max}$ is the maximum allowable neutral line voltage.

6) Branch current constraints

For the branch current $I_{ij,t}$, it is still expressed in complex form:

$$I_{ij,t}=Y_{ij}V_{ij,t}=Y_{ij}\left(V_{i,t}-V_{j,t}\right) \tag{18}$$

$$Y_{ij}=G_{ij}+jB_{ij} \tag{19}$$

$G_{ij}$ and $B_{ij}$ are the conductance and the conductance of the line $ij$, respectively. Therefore, the original equation can be transformed into:

$$\left|I_{ij,t}\right|=\left|Y_{ij}\right|\left|V_{ij,t}\right|=\sqrt{G_{ij}+jB_{ij}}\cdot\sqrt{\left(V_{i,t}^{real}-V_{j,t}^{real}\right)^2+\left(V_{i,t}^{imag}-V_{j,t}^{imag}\right)^2} \tag{20}$$

Squaring both sides of the above equation and removing the root sign further convexifies the formulation, and finally, the branch current constraint can be optimized as:

$$\left|I_{ij,t}\right|^2 \le \left(I_{ij}^{\max}\right)^2 \tag{21}$$

### 2.1.2 User-side optimization model

(1) Objective function

According to the user's most good economic cost, the model that user optimizes is established. The establishment of the target function which expresses the user's interest on a specific node is given as below:

$$\max f_i = \sum_{\varphi\in\Phi} C_{i,\varphi}^{G} + \sum_{\varphi\in\Phi} C_{i,\varphi}^{DR} - \sum_{\varphi\in\Phi} C_{i,\varphi}^{ESS} \tag{22}$$

$\Phi$ is the set of three phases; $C_{i,\varphi}^{DR}$ is the benefit of user response regulation, $C_{i,\varphi}^{ESS}$ is the cost of charging and discharging the user's ESS; and $C_{i,\varphi}^{G}$ is the cost of purchasing or selling power to the user revenue:

$$C_{i,\varphi}^{G} = \begin{cases} \gamma_t^{buy} \sum_{t=1}^{T} P_{i,\varphi,t}^{G} \Delta t, & P_{i,\varphi,t}^{G} < 0 \\ \gamma_t^{sell} \sum_{t=1}^{T} P_{i,\varphi,t}^{G} \Delta t, & P_{i,\varphi,t}^{G} > 0 \end{cases} \tag{23}$$

$P_{i,\varphi,t}^{G}$ is the power purchased or sold by the user to the grid company; $\gamma_t^{buy}$ is the purchase price; $\gamma_t^{sell}$ is the price of the sale of the power; $\Delta t$ is the time interval; and $T$ is the total time duration.

$$C_{i,\varphi}^{DR} = \varepsilon_{i,\varphi,t} \sum_{t=1}^{T} P_{i,\varphi,t}^{DR} \Delta t \tag{24}$$

$\varepsilon_{i,\varphi,t}$ is the price of additional incentives for the user to respond to regulation; $P_{i,\varphi,t}^{DR}$ is the power of the user to respond to regulation.

$$C_{i,\varphi}^{ESS} = \eta_s \sum_{t=1}^{T} \left(P_{i,\varphi,t}^{char} + P_{i,\varphi,t}^{disc}\right) \Delta t \tag{25}$$

$$\eta_s = \frac{C_s^{P,ESS}}{2E_s^{ESS}} \tag{26}$$

$P_{i,\varphi,t}^{char}$ and $P_{i,\varphi,t}^{disc}$ are the charging and discharging power of the ESS, respectively; $\eta_s$ is the charging and discharging cost of the ESS (the unit cost of charging and discharging is the same); $E_s^{ESS}$ is the capacity of the ESS of type $s$ .The operating cost of a complete charge/discharge of the ESS is calculated as follows:

$$C_s^{P,ESS} = \frac{C_s^{capital}}{N_s^{ESS}(x)} \tag{27}$$

$C_s^{capital}$ is the investment cost of the EES; $N_s^{ESS}(x)$ is the total number of charge/discharge cycles of the EES, which is determined by the charge/discharge depth $x$.

(2) Constraints

1) Power balance constraint

$$P_{i,\varphi,t}^{G} = P_{i,\varphi,t}^{LOAD} - P_{i,\varphi,t}^{TR} - P_{i,\varphi,t}^{PV} - P_{i,\varphi,t}^{ESS} \tag{28}$$

$P_{i,\varphi,t}^{LOAD}$ is the user's load; $P_{i,\varphi,t}^{TR}$ is the user's adjustable load; $P_{i,\varphi,t}^{ESS}$ is the EES charging or discharging power.

2) Energy storage system constraints

The SOC constraint of ESS is:

$$S_{i,\varphi,t+\Delta t}^{SOC} = S_{i,\varphi,t}^{SOC} + \frac{P_{i,\varphi,t}^{char}\eta_s^{char}\Delta t}{E_s^{ESS}} - \frac{P_{i,\varphi,t}^{disc}\Delta t}{\eta_s^{disc}E_s^{ESS}} \tag{29}$$

$S_{i,\varphi,t}^{SOC}$ and $S_{i,\varphi,t+\Delta t}^{SOC}$ are the SOC of the stored energy at the moments of $t$ and $t+\Delta t$, respectively; $\eta_s^{char}$ and $\eta_s^{disc}$ are the charging and discharging efficiencies of the ESS, respectively.

$$S_{\min}^{SOC} \le S_{i,\varphi,t}^{SOC} \le S_{\max}^{SOC} \tag{30}$$

$$\begin{cases} 0 \le P_{i,\varphi,t}^{char} \le P_{i,\varphi,t}^{char\max} \\ 0 \le P_{i,\varphi,t}^{disc} \le P_{i,\varphi,t}^{disc\max} \end{cases} \tag{31}$$

$S_{\max}^{SOC}$ and $S_{\min}^{SOC}$ are the upper and lower bounds of the energy storage SOC, respectively; and $P_{i,\varphi,t}^{char\max}$ and $P_{i,\varphi,t}^{disc\max}$ are the maximum values of the charging and discharging power of the ESS, respectively.

3) Power constraints for adjustable loads

$$0 \le P_{i,\varphi,t}^{TR} \le P_{i,\varphi,t}^{TR\max} \tag{32}$$

$P_{i,\varphi,t}^{TR\max}$ is the upper limit of user adjustable load.

### 2.1.3 Chaotic particle swarm based solution method

After the collaborative optimization model between the grid side and the user side is built, because it relates to a nonlinear optimization problem that has many variables and constraints, this paper puts forward the chaotic particle swarm optimization algorithm to solve the model and obtain the best economic dispatching under the system operation constraints.

Chaos is named as the non-deterministic random movement condition which is got from definite equations. The variables that are inside these equations and are in chaotic state are called chaotic variables. One quite famous chaotic system is the Logistic equation.

$$y_{n+1} = \mu y_n\left(1-y_n\right)\left(n=0,1,2,\cdots;0\le\mu\le 4\right) \tag{33}$$

where $\mu$ is the control parameter and $n$ is the number of iterations. The experiment proves that when $\mu$ increases to $3.58 \le \mu \le 4$, the period of change of the equation value becomes infinite, so that the solution of the equation is uncertain at each iteration. At this time, the Logistic equation becomes a chaotic system.

The concept of chaotic optimization is be put into the particle swarm optimization algorithm, hence leading to the generation of the chaotic particle swarm optimization algorithm (CPSO). In the optimization algorithm of chaotic particle swarms, for avoiding the stagnation of some particles in the iteration process, the algorithm can utilize the traversal property of chaotic variables. It produces a disordered sequence step by step according to the present whole optimal position which is discovered by the particle swarm. After that, the position of a single particle inside the present particle group is randomly used to replace the optimal particle position inside the order, and therefore the iteration goes on further. This method solves the problem of early convergence of the algorithm which is brought about by particle stagnation.

Below we carry out the elaboration of the concrete operation steps of the chaotic particle swarm optimization algorithm:

(1) Determine the parameters of the algorithm, randomly generate a population of $N$ particles, and initialize the particles.

(2) Carry out the modification on the velocity and position of the particles according to the basic renewal formulas (34) and (35) which belong to the particle swarm algorithm.

$$v_i^{k+1} = \omega v_i^k + c_1 r_1 \left( x_{pbest}^k - x_i^k \right) + c_2 r_2 \left( x_{gbest}^k - x_i^k \right) \tag{34}$$

$$x_i^{k+1} = x_i^k + v_i^{k+1} \tag{35}$$

(3) Chaotic optimization of the particle swarm optimal position $x_{gbest}^k$:

1) Mapping $x_{gbest}^k$ to the domain of definition $[0,1]$ of the Logistic equation via equation (36):

$$y_1^k = \frac{x_{gbest}^k - R_{\min}^k}{R_{\max}^k - R_{\min}^k} \tag{36}$$

2) Perform $M$ iterations for $y_1^k$ through the Logistic equation $y_{n+1}^k = \mu y_n^k \left(1 - y_n^k\right)$ to obtain the chaotic sequence $y^k = \left( y_1^k, y_2^k, \cdots, y_M^k \right)$.

3) Employ the below-given equation to carry out an inverse mapping of the chaotic sequence back to the original solution space:

$$x_{gbest,m}^{*k} = R_{\min}^k + \left( R_{\max}^k - R_{\min}^k \right) y_m^k \text{ , } m = 1, 2, \cdots, M \tag{37}$$

This produces a sequence of chaotic variable feasible solutions: $x_{gbest}^{*k} = \left( x_{gbest,1}^{*k}, x_{gbest,2}^{*k}, \cdots, x_{gbest,M}^{*k} \right)$.

4) Carry out calculation of the fitness value for each feasible solution vector that lies inside the group of feasible solutions. Then, we retain the feasible solution vector which corresponds to the example when the fitness value attains its optimal value. This specific vector is named as $x_g^{*k}$.

(4)Randomly select one particle from the already existing particle group, and use the position vector of $x_g^{*k}$.

(5)Just go forward to step (2), until the algorithm either reaches the maximum iteration count or obtains a solution that is sufficiently satisfying.

## 2.2 Strategies for station autonomy with synergistic energy storage and PV

For further enhancing the working independence and voltage stability of low-voltage distributed photovoltaic (PV) systems, this research proposes a cooperation control method between energy storage and PV. This method combines the flexible change ability of the energy storage system and the inactive power support characteristic of the photovoltaic inverter. Through this method, it causes the station area to attain the most excellent operation state under the conditions that the voltage surpasses the limit value and power unbalanced condition exists..

### 2.2.1 Voltage control of energy storage pairs based on coordinated control scheme for optical storage

We carry out contemplation on the incorporation of a Battery Energy Storage System (BESS) into the low-voltage part of the country-side distribution electric network. Use the centralized energy storage method to provide a unified power supply on the low-voltage side of the transformer.Distributed photovoltaic power generation prioritizes power supply to loads within the station area $P_{load}$, $P_{PV}$ represents the output of the photovoltaic power generation system; When surplus appears, the extra electric energy can be transmitted to the main electric grid through the conducting bus. Oppositely, when the power output of the photovoltaic system is low and the load requirement is high, the main power grid provides electric power to the bus bar. The $P_{PV}$ represents the excess power and the $P_{low}$ represents the compensation power. Therefore, the excess power and the compensated power can be called the active exchange power between the distribution system and the main grid. Using $\Delta P$ to represent the active load and difference between the PV output and the station can be expressed as:

$$\Delta P = P_{PV} - P_{load} \tag{38}$$

In the load's low valley time period $t$, the below flow is utilized to confirm the working condition of the energy storage equipment. It depends upon the large degree of the load and the electric quantity holding state (SOC) of the energy storing device:

$$\begin{cases} \begin{cases} \Delta P(t) > P_{high(m)} \\ SOC(t) < SOC_{(\max)} \end{cases} = 1 \\ \begin{cases} \Delta P(t) > P_{high(m)} \\ SOC(t) > SOC_{(\max)} \end{cases} = 1 \end{cases} \tag{39}$$

where $P_{high(m)}$ is the charging power threshold; $SOC_{(\max)}$ is the maximum stage of the charging status of the energy-storage apparatus is the thing that is being spoken of. $SOC$ it expresses the ratio of the still left battery capacity against the whole battery capacity, shown in a percentage form.. The value range is 0~1, when $SOC = 0$ that the battery has been completely discharged, when $SOC = 1$ that the battery is completely full. Under the situation that the load lies at its lowest position, the exchanged power exceeds the charge upper bound, or the residual electric quantity is not sufficient, the energy storage equipment will carry out the

charge procedure. On the opposite side, if the above conditions are not satisfied, the state of charge and discharge still does not have any change.

After the energy storage equipment on the low voltage side of the transformer which is inside the distribution network has been accessed, the energy storage system bears the management and the calculation of the real-time power difference. After that, it sends out power order documents to the energy storage unit to adjust its charge and discharge working processes. Furthermore, the capability of this system may be configured through a flexibly way. In the processes of charging and discharging of the unit, the power redistribution can be conducted in accordance with the proportion of the remaining capacity to the chargeable remaining capacity of the whole energy storage system.

The energy storage is mainly used to solve the problems of over-voltage and under-voltage that appear on the side of consumers. This system carries out a time-divided input control method. In the course of one single cycle, the energy storage device receives $P_{high}$ and compensates $P_{low}$, It carries out the function that peak cutting and valley filling are realized. When the electric energy produced by the photovoltaic system has a very big exceedance over the load requirement, and the difference between them is larger than $R_1$, the energy storage device starts the charging procedure and stores the extra energy in the energy storage battery. Under the circumstances that the photovoltaic (PV) generated electricity is obviously lower than the load requirement, the difference is smaller than $P_2$, the energy storage device discharges, and inputs the energy from the storage battery into the power grid.

When undervoltage situation appears inside the distribution station area, the compensation work is implemented by means of the energy storage system's discharge behavior. The discharge capability of this system is equal to the capability of the energy storage device that is used in overvoltage control actions. The work condition of the energy storage equipment is being confirmed through the below equation:

$$\begin{cases} \begin{cases} \Delta P(t) < P_{low(m)} \\ SOC(t) > SOC_{(\min)} \end{cases} = 0 \\ \begin{cases} \Delta P(t) < P_{low(m)} \\ SOC(t) < SOC_{(\min)} \end{cases} = 0 \end{cases} \tag{40}$$

where $P_{low(m)}$ is the discharge power threshold; $SOC_{(\min)}$ is the lower limit of the load state of the energy storage device. When the exchange capability is smaller than the pre-set threshold and the residual capacity surpasses the maximum limit, it is the energy storage unit that will carry out the discharge action. Under the situations that these conditions have not been satisfied, the former working state will hence be kept.

### 2.2.2 Inverter Reactive Margin Assessment

Carrying out an assessment work of the reactive allowance for inverters has very important meaning in the stability research of electric power systems. This point is especially important when we carry out assessment on electric power quality within low-voltage areas. The main advantages that come from conducting this kind of reactive margin evaluation are enumerated herein below:

(1) Inverter reactive margin assessment helps to prevent voltage collapse and voltage instability events and ensure voltage stability.

(2) The assessment of reactive margin is essential for power system planning and daily operation management, and can guide reactive power compensation equipment.

(3) It possesses the ability to provide a sufficient quantity of reactive power support, which thus can effectively promote the entire reliability of the system.

If the PV grid-connected active power at a node reaches the upper limit value while the load is at a lower level, the net power value at that node will be approximately equal to the maximum value, and the voltage may cross the limit at any time. The use of reactive power margin assessment for advance judgment can effectively avoid the occurrence of voltage crossing the upper limit.

$$\delta^{OV} = \frac{U_i^{MAX} - U^{tk-OV}}{\left| \sum_{j=1}^{i} S_{i,j}^{V-2} \sqrt{S_j^2 - \left( P_{PV,j}^{rated} \right)^2} \right|} \tag{41}$$

where $\delta^{OV}$ is the test coefficient of reactive margin; $U_i^{MAX}$ is the maximum voltage reached at node $i$; $U^{tk-OV}$ is the upper limit of the voltage operating range, which is taken to be $1.05\,pu$ in this paper; $S_j$ stands for the capacity of the photovoltaic inverter at node $j$; $P_{PV,j}^{rated}$ is the rated grid-connected power of node $j$. When the test coefficient is greater than 0, it indicates that the reactive power capacity is insufficient, and vice versa, it indicates that the reactive power capacity is sufficient.

### 2.2.3 Optical storage cooperative control strategy process

Fig. 1 shows the strategy flow of cooperative control of PV and energy storage based on intelligent fusion terminal.

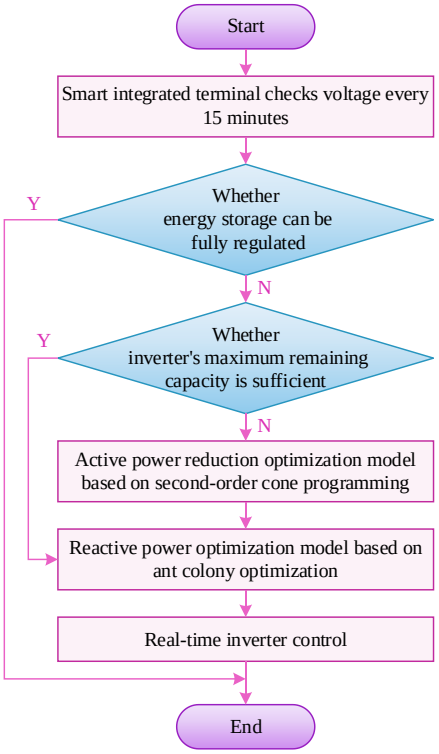


*Figure 1: The strategy of coordinated control of photovoltaic and energy storage*

Use the intelligent integration terminal to collect the station region data at every 10-minute gaps. Next, you need carry out assessment on whether the voltage has exceeded the upper limit of voltage or has dropped under the lower limit of voltage. Under the circumstance that the voltage goes beyond these threshold values, we should give the priority to arranging energy storage for charging for the adjustment of the voltage. When the energy storage hold capacity is sufficient, therefore we rely on the energy storage to carry out regulation work. When the energy storage ability is not enough, therefore carry out evaluation on the reactive power margin that the photovoltaic inverter has. If this margin is enough, the voltage adjustment can be realized through the reactive power that the inverter possesses. When the storage ability has been verified to be not enough, an evaluation on the reactive power of the photovoltaic (PV) inverter is conducted by us. On the opposite side, when the storage capability is enough, the reactive power of the inverter can be utilized by people to control the voltage that is inside the station region. The designing of coordinated controller parameters can guarantee the efficacy which voltage control has. Under the situations when the evaluation of the network's reactive power margin is not enough, therefore the priority is given by us to using the inverter's reactive power for voltage adjustment in the station region. After the reactive power margin has arrived at its limit, the reactive power of PV is by degrees decreased. This procedure targets to release the needed capability for the inverter's inactive power control inside voltage adjustment. In this research article, the chaotic particle swarm method which was spoken of above is used by us to further carry out optimization on the adjustment of voltage by means of reactive and active power.

# 3 Assessment of the effects of voltage regulation, power synergies and station autonomy

For the verification of the specific regulation influence of the low-voltage (LV) distribution network energy regulation model which is based on CPSO optimization and the photovoltaic (PV) storage synergistic strategy that this paper has researched and formulated on the grid-connected operation of distributed energy resources (DERs) within the distribution network, this research uses the 24-hour operation data of a real distributed PV system to construct a simulation model of the LV distribution network. After that, this text carries out quantitative evaluation on the effect of this strategy from many dimensions, which include the total promotion of voltage quality, the cooperative control of active power and reactive power, and the cooperative reaction inside the station region.

## 3.1 PV System Load Profile

In this paper, 24h actual operation data of distributed PV system is used as DER output data. The on-load voltage regulator transformer is divided into 9 stalls, and each stall is adjusted by 0.01 pu; the capacitor bank has 6 groups, and the single group has a switching capacity of 0.05 Mvar.Fig. 2 demonstrates the 24-hour load characteristic curve of the PV system.

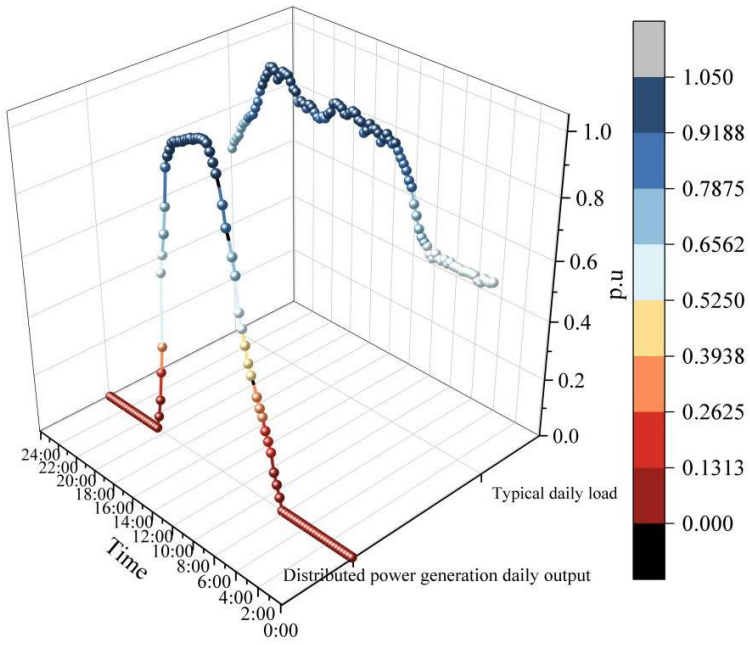


*Figure 2: The 24-hour load characteristic curve of this photovoltaic power station*

The load vs. output graph shows that the output of the PV plant starts from 6:30 and has active output between 18:30 in the afternoon, and it cannot continue to output active power without light at other times, hence, the combined running of photovoltaic (PV) and energy storage, which is put forward in Section 2.3, is utilized to solve the defect of the PV power station possessing an output of 0 per-unit (p.u.) in the night time. Even when sunlight does not exist, the distributed photovoltaic can still maintain a continuous power output that lies between 0.62 and 0.67 per unit.

## 3.2 Evaluation of the effectiveness of synergistic control strategies based on SVA and power factor

The study examines the cooperative control strategies for photovoltaic storage in a simulated low-voltage distribution network environment. According to the 24-hour data that we got from the above-mentioned actual photovoltaic (PV) power station, many different working situations are built. The aim of the present text is to evaluate the whole effect of the strategy in the promotion of voltage quality.

### 3.2.1 Comparative analysis before and after DER participation in distribution network voltage optimization and control

Split the above 24 hours into 96 sampling points. And 24 grid-connected nodes are selected to be studied and analyzed to define the voltage average offset index SVA for each sampling point.

In addition, three states exist of distributed power sources which are not connected to the electric grid, and grid optimization work is performed completely according to the multi-period cooperative optimization control model (MPCO), and optimization based on the model optimization under chaotic particle swarm algorithm and applying the cooperative control strategy of energy storage and photovoltaic optimization (MPCO+CPSO+PES) are selected. The SVA analysis is performed on 96 sampling points in these three states, and Fig. 3 demonstrates the SAV voltage offset index curves for the three cases.

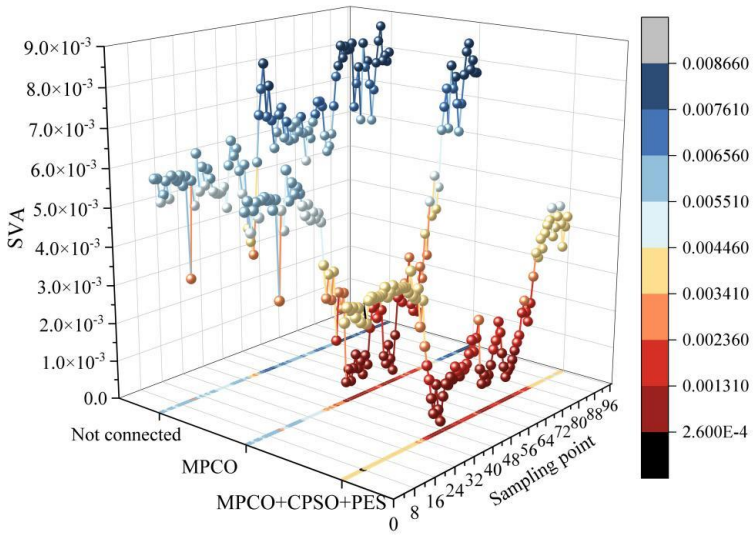


*Figure 3: The curves of the SAV voltage offset index under three conditions*

Only inside the single multi-time combined optimization model, the average numerical value of SVA is 4.10×10 - 3. This numerical result is 35.5 percent smaller than the result in the condition that distributed electric power does not get linked to the power grid. This indicates that in the energy regulation model of the low-voltage distribution network, voltage fluctuation can be effectively restrained through the cooperation of energy storage, SVG, and flexible loads. Furthermore, this present paper has combined the chaotic particle swarm algorithm (CPSO) together with the optical storage cooperative control strategy, and the effect is even more outstanding. the average value of SVA is further reduced to $2.66\times10^{-3}$, which is 35.1% lower than that of using only the multi-timescale cooperative optimization model, and the maximum value of SVA is compressed significantly from $8.50\times10^{-3}$ to $4.65\times10^{-3}$, which indicates that for the time period when the voltage is most likely to exceed the limit (sampling point 80-96 corresponds to the evening and nighttime hours), the optimization method incorporating the storage-PV cooperative control strategy has stronger suppression capability.

Specifically, the grid optimization based only on the multi-temporal cooperative optimization control model has about the same average voltage offset SVA at the sampling points 0-32 and 80-96 (i.e., 0:00-6:30 and 18:30-12:00 no-lighting time) and when distributed power sources are not connected to the grid, which indicates that pure multi-temporal optimization has limited regulating capability when PV is not producing power. And after applying storage PV cooperative control strategy optimization in each sampling point SVA has decreased, through CPSO optimization scheduling, and combined with inverter reactive margin assessment and storage dynamic casting, so that the SVA curve is always at a lower level, in the night time hours according to the SOC and voltage state of the discharge support, to achieve the no-light is also regulated. Meanwhile, during the dual peak hours of midday load and PV output (sampling points 32-72), the voltage offset is controlled in a lower range.

### 3.2.2 Analysis of the effect of DER participation in voltage regulation at different power factors

It is known that the multi-time co-optimization model + CPSO + optical storage co-optimization method works on voltage stabilization, and now we turn to the analysis of the DER voltage regulation effect under different power factors under this method. Keeping the total capacity of DER unchanged, the average voltage offset indexes of each node of the whole simulation

system when running with different power factors (cos φ=0.9, 0.925, 0.95 and 0.975) are used. Fig. 4 demonstrates the SVA values at each sampling point for different power factors.

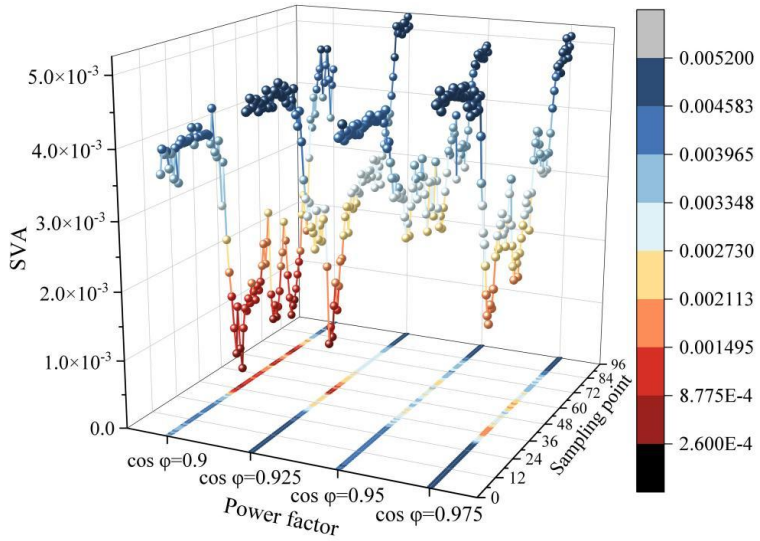


*Figure 4: The SVA values at each sampling point for different power factor levels*

When the power factor is been adjusted to 0.95, the system can show the most stable voltage characteristic in the majority time of one day. In the daytime peak time interval (from 9:00 to 19:00), wherein the number of sampling points lies between 36 and 76 and the photovoltaic (PV) output is comparatively high, a power factor of cos φ = 0.95 leads to a lower apparent power variation (SVA) value that is about 0.003. This numerical result is commonly lower when we compare with setups that use other power factors, therefore it shows a comparatively stronger voltage regulation capability.No matter if the power-factor has deviation from 0.95, no matter it becomes larger or smaller, the voltage offset of the distribution network has a steady rise. When the reactive power that has an excessive quantity enters the distribution network, it brings about an over-rising of the system voltage level. On account of this circumstance, the numerical value of the average voltage offset index SAV gradually has an increase. The research results show that in the cooperative control system that this paper puts forward, the power factor has no need to be maximized. On the contrary, the setting of cos φ as 0.95 is a more appropriate choice, because it can carry out the balance between reactive power support and voltage stability. Based on the concept of inverter reactive power margin assessment which was put forward in the foregoing section, through properly setting the power factor and fully utilizing the reactive power adjustment ability of Distributed Energy Resources (DER), the voltage independence of the station region can be further promoted without obstructing active power output.

## 3.3 Active-reactive power cooperative voltage control regulation analysis

After we have confirmed the overall influence of this strategy, we therefore will now go more deeply into the regulation core. We shall complete this work through selecting a representative feeder together with its 24 consumer nodes. Next, we shall respectively research the direct effect of active power adjustment (to be specific, directly limit the photovoltaic power output) and reactive power adjustment (change the inverter power factor) on each node's voltage. In this research work, the B-phase voltage is taken to be an illustrative example.

### 3.3.1 Effectiveness of active power regulation applications

Select a typical day at noon time on the photovoltaic inverter cluster active power for batch voltage drop, statistics of each node voltage, distribution transformer reverse load rate changes, and analyze the photovoltaic inverter group control group regulation field application effect. The transformer reverse active power is 207.49kW, the reverse load rate is 103.09%, and the voltage of each node shows the change rule of gradually increasing from the station side to the end of the line.

The active power limit is got through multiplying the rated active power of photovoltaic (PV) inverters by a special proportion. After that, according to the control instruction of the active limit that the cloud main station of the electric network dispatching system issues to the PV current transformer groups, the active power of all PV current transformers inside the station region is adjusted. Detailed measured data of voltage at each node and distribution inverter reverse load ratio are measured under different control commands at full PV power generation state and at 75%, 50%, 25% and 5% of the active output limit, respectively.

In this paper, the general overvoltage threshold U1 is defined as 243 V, and the severe overvoltage threshold U2 is 250 V. The B-phase voltages at 24 nodes under different active regulation commands are shown in Fig. 5.

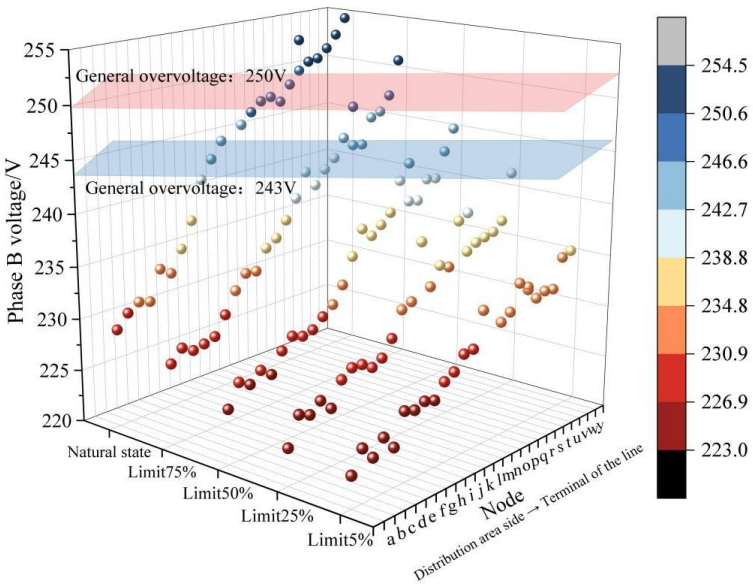


*Figure 5: The B-phase voltages of 24 nodes under different active control instructions*

Under the natural state of full PV power generation at noon, six nodes are in the state of severe overvoltage (>250 V), including t, u, v, w, s, and y, which are at the end of the line. Starting from node j (243.17 V), the subsequent nodes, k, l, m, n, o, p, q, r, and s, and other nine nodes are in the state of general overvoltage (>243 V). The voltage is effectively suppressed when the active output of the PV cluster is limited by issuing a regulation command. At 75% of the limit, the severe overvoltage nodes are basically eliminated, and only the terminal y node (250.87V) is left slightly exceeding 250V; the general overvoltage nodes are also greatly reduced, mainly focusing on the n, o, p, q, r, s, and y at the very end, and the remaining 16 nodes are in a safe state of <243V. All node voltages fall back to below 250V at 50% of the limit, and no severe overvoltage exists. Only the y node, which exists at the very end, is 244.93V, slightly above the general overvoltage threshold. When the active output limit is set to 25% and 5% of the rated value, the voltage is further smoothed and all node voltages fall below the general overvoltage threshold of 243V, and all node voltages in the station area are in a safe

operating condition.

### 3.3.2 Effectiveness of reactive power regulation applications

The application of power factor change for the adjustment of reactive power is utilized. Just like what Figure 6 shows, the B-phase voltages on the nodes are measured under different control commands when a completely active power generation condition exists. This measurement is implemented when the power factor is respectively set to 1, 0.975, 0.95, 0.925, and 0.9.

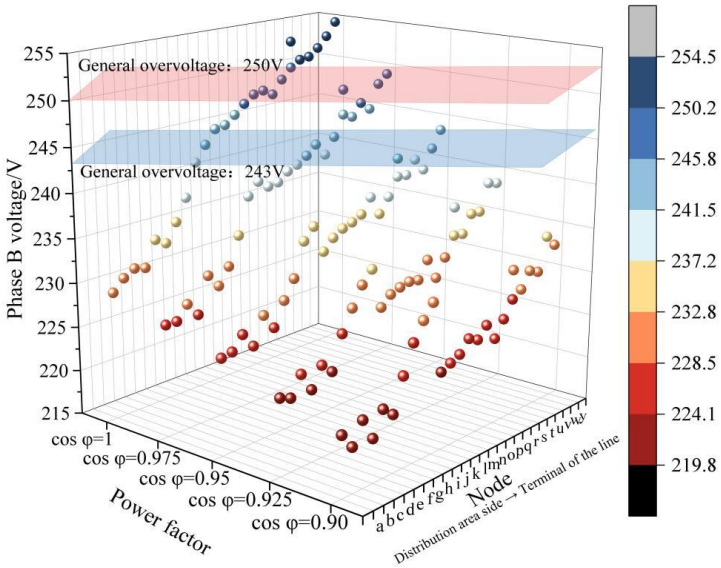


*Figure 6: The B-phase voltages of 24 nodes under reactive power control instructions*

In the purely active generation state with a power factor of 1, the voltage situation is consistent with the natural state of Fig. 5, where the voltage at node y at the end of the line is as high as 254.41 V. The nodes t, u, v, w, s, and y are in the state of severe overvoltage (>250 V), whereas the numerous nodes from node j backward are in the state of general overvoltage (>243 V). When the power factor is reduced and the inverter is allowed to emit reactive power, the voltage level improves. When the power factor is reduced to 0.975, only w, s, and y exist at the severe overvoltage nodes, and the voltage at the terminal y node is reduced from 254.41V to 249.06V, and the voltage at the grid-connected points of all the PV inverters decreases by an average of 4.37V compared to the state of purely active and natural generation, which is a significant effect. When the power factor is further reduced to 0.95, all node voltages have been below 250V, and there is no serious overvoltage situation, leaving only the most terminal y-node (243.48V) slightly exceeding the general overvoltage threshold. At power factors of 0.925 and 0.9, all node voltages have dropped below 243V, completely eliminating overvoltage. The reactive power output that comes from the PV inverter can specifically counteract the voltage drop which is in the line. This kind of pointed compensation has very high efficiency in holding back the growth of end voltage.

## 3.4 Effectiveness of real-time autonomy of stations

### 3.4.1 Response of stations under 10kV Ping'an Line to active regulation commands

At present, the station-level PV group control system is mainly used to solve the problem of feeder heavy overload. Take the 10kV Ping'an line in the jurisdiction as an example, the

maximum annual reverse current of the station is 378.18A, the rated line current-carrying capacity is 425A, and the maximum load ratio is 94.07%. In order to manage the line reverse overload problem, at 10:00 (sampling point 41), the cloud master station sends out an active regulation command, and the intelligent fusion terminal of each station under the jurisdiction of 10kV Ping'an line receives the power regulation command and decomposes it to each PV inverter, and the power curve of the station is shown in Figure 7.

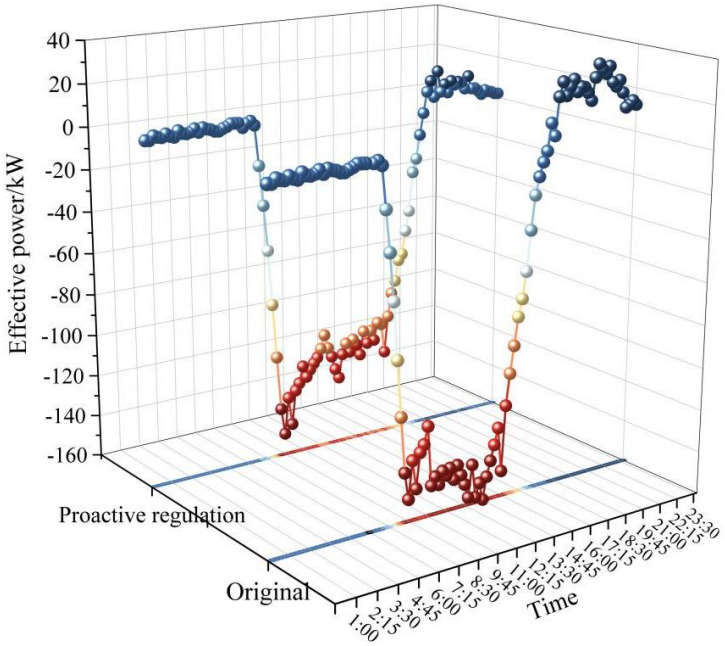


*Figure 7: The response of the distribution area to the active power control instructions*

Before the regulation instruction is issued (0:00-9:45), the power curve of the station area shows a weak positive power at night, which represents the power taken from the grid, and from 7:00 when the PV starts to produce power, the power quickly turns to negative value (back-feeding power to the grid), and the raw reverse power is as high as -156.72 kW at around 12:30 p.m. And when the regulation instruction is issued, the curve is in the light period after 10:00 p.m. The curve shifted upward significantly, and the reverse power was suppressed with a reduction of between 15% and 30%. The feeder reverse current decreases by 117.39A and the reverse load ratio decreases to about 58.39% after the regulation instruction is given. Effectively solve the distribution network balance control and local heavy overload problems. The regulation impact still exists when the power is positive grid pickup after 17:45, and the positive power value of the user's power consumption - PV output is also generally reduced, and even part of the time still maintains a weak reverse power feeder state (negative value). The regulation strategy smoothed the net power exchange curve between the station and the main grid to some extent.

### 3.4.2 Voltage comparison before and after station node optimization

Based on section 2.3.2 it is known in this paper that for $U_i^{MAX}$ voltage operating range upper limit value is $1.05pu$, 24 nodes and 96 sampling points in the station area are optimized in the grid optimization based on the Multi-Period Cooperative Optimization Control (MPCO) model only and model optimization based on the Chaotic Particle Swarm Algorithm under the Chaotic Particle Swarm algorithm and applying the storage PV Cooperative Control Strategy Optimization (MPCO+CPSO+). PES) voltages before and after optimization are shown in Fig.

8, Fig. 9 and Fig. 10, respectively. The images are contour plots of voltage at different nodes and sampling points in the three states (96 sampling points in 24 hours on the horizontal axis and 24 node data on the vertical axis), with the color mapped to the voltage magnitude. The two subplots are voltage profiles at sampling point 48 and node m, respectively. The more the color tends to blue indicates the higher voltage, and it can be found that the red region in Fig. 10 accounts for most of the area, indicating that the MPCO+CPSO+PES optimization strategy has the best effect of voltage control in the platform area.

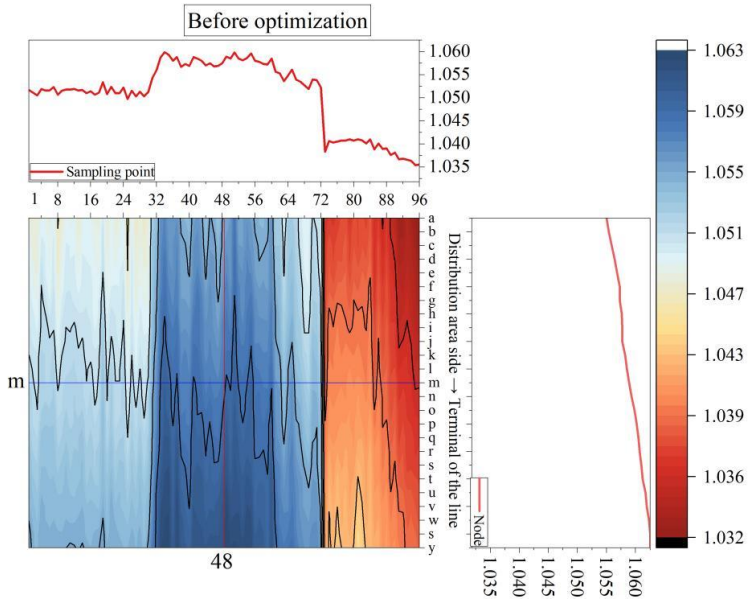


*Figure 8: Voltage distribution before optimization*

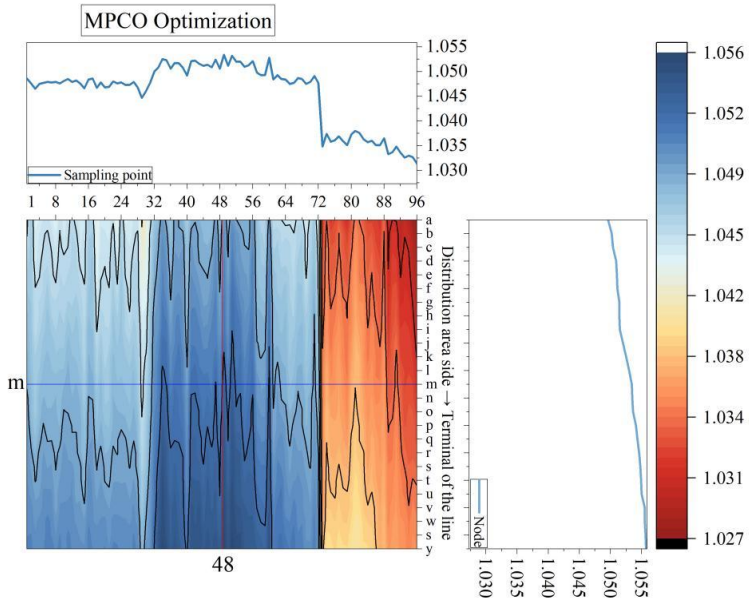


*Figure 9: Voltage distribution after MPCO optimization*

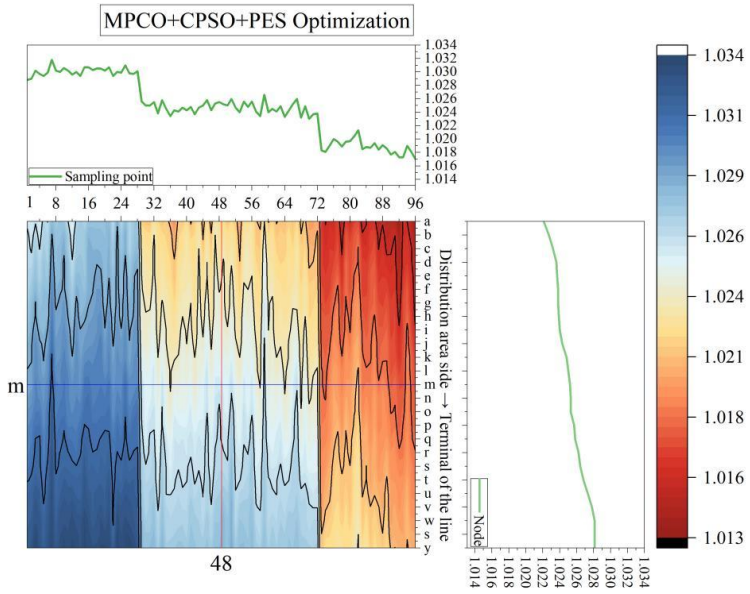


*Figure 10: Voltage distribution after MPCO+CPSO+PES optimization*

Before optimization, the voltage passing rate is only 65.17%, more than one-third of the sampling points have voltage >1.05 p.u., and the highest voltage reaches 1.063 p.u., which is a risk of voltage overrun. After the initial adjustment of the multi-time co-optimization model (MPCO), the qualification rate is increased to 86.92%, and the highest voltage is reduced to 1.056 p.u. The overall situation is greatly improved, but there are still some nodes operating under pressure. And finally, after adopting the strategy of integrating chaotic particle swarm algorithm and optical storage synergy, the voltage qualification rate reaches 100%, and the maximum voltage is within the safety range of 1.029 p.u., realizing the voltage autonomy of the station area.

From the time dimension (i.e., sampling points), taking the m-node as an example, the voltage curve before optimization is generally elevated during the PV big hairy hours from 7:00 to 17:00, with a large number of sampling points exceeding the 1.05 p.u. threshold.After MPCO optimization, the curve wave peaks are much smoothed out (the blue curve on the upper left of Fig. 9), but there is still a slight overrun in the lunchtime peak hours from 12:00 to 13:00. By the time the whole voltage curve wave amplitude is smaller after integrating the optical storage synergistic strategy, the maximum and minimum voltages are 1.016 p.u. and 1.032 p.u., respectively, and the voltage of the station area is anchored within the safe range under this optimization strategy.

Analyzing from the spatial dimension (24 nodes a→y), at the sampling point of 48, which corresponds to the moment of 12:00 noon, the profiles of the sampling points in the lower right corner of the three contours all show an incremental curve from the top to the bottom and from the left to the right, i.e., the voltage shows a step-by-step increase from the station side (node a) to the end of the line (node y).

# 4 Conclusion

The study synergistically models the grid-side loss reduction and user-side economic objectives, empowers the system with intelligence through chaotic particle swarm algorithms, and empowers the system with agile execution capability through synergistic control strategies, realizing to active autonomy.

In the present research paper, a three-stage control method is utilized by us. This strategy is

constituted by putting energy storage in first place, providing reactive power support, and decreasing active power. Through making adjustment of the power factor of the photovoltaic (PV) inverter to 0.9, it is successfully enabled to bring the voltage of the over-voltage node which is at the end of the line back from 254.4V to the safe scope of 232.7V. In addition, in the time of midday peak, the setting of active output limit on 50% makes all node voltages be able to drop below the critical over-voltage threshold which is 250V.

After receiving the command from the cloud master station, the reverse power of the stations under the 10kV Ping'an Line was reduced from -146.1kW to -123.4kW at 10:00 a.m., and continued to reduce the reverse current by about 20-30kW in the following hours. Resolving the risk of heavy overload with line load ratio as high as 94.07%.

# About the Authors

Guocheng Li, born in 1977, from Zibo, Shandong Province, master's degree from Shandong University of Science and Technology. He is currently working in State Grid Dezhou Power Supply Company, specializing in electrical engineering and automation.

Cong Wang, born in 1988, from Dezhou, Shandong province, bachelor degree from Northeast Electric Power University, currently working in State Grid Dezhou Power Supply Company, research direction is electrical engineering and automation.

Zeguang Lu, born in 1985, from Dezhou, Shandong Province, bachelor degree from Changsha University of Science and Technology. He is currently working in State Grid Dezhou Power Supply Company. His research direction is electrical engineering and automation.

Ze Zhang, born in 1990, from Dezhou, Shandong province, master's degree from North China Electric Power University. He is currently working in State Grid Dezhou Power Supply Company, specializing in electrical engineering and automation.

Xiaoran Li, born in 1988, from Dezhou, Shandong Province, bachelor degree from Qingdao University of Science and Technology, currently working in State Grid Dezhou Power Supply Company, research direction is electrical engineering and automation.

Xiaoqin Wang, born in 1984, from Dezhou, Shandong province, bachelor degree of Liaocheng University, currently working in Sichuan Changduo Electric Power Engineering Co., Ltd., research direction is electrical engineering and automation.

# References

[1] Castellanos-Sosa, F. A., Cabral, R., & Mollick, A. V. (2022). Energy reform and energy consumption convergence in Mexico: A spatial approach. Structural Change and Economic Dynamics, 61, 336-350.

[2] Han, J., & Chang, H. (2022). Development and opportunities of clean energy in China. Applied Sciences, 12(9), 4783.

[3] Caineng, Z. O. U., Feng, M. A., Songqi, P. A. N., Qun, Z. H. A. O., Guoyou, F. U., Yichao, Y. A. N. G., ... & Hanlin, L. I. U. (2023). Global energy transition revolution and the connotation and pathway of the green and intelligent energy system. Petroleum Exploration and Development, 50(3), 722-740.

[4] Chai, Y., Guo, L., Wang, C., Zhao, Z., Du, X., & Pan, J. (2018). Network partition and voltage coordination control for distribution networks with high penetration of distributed PV units. IEEE Transactions on Power Systems, 33(3), 3396-3407.

[5] Gill, A., Choudhary, A., & Bali, H. (2021). Renewable distributed generations optimal penetration in the distribution network for clean and green energy. Asian Journal of Water, Environment and Pollution, 18(2), 37-43.

[6] Jiang, S., Wan, C., Chen, C., Cao, E., & Song, Y. (2018). Distributed photovoltaic generation in the electricity market: status, mode and strategy. CSEE Journal of Power and Energy Systems, 4(3), 263-272.

[7] Rahdan, P., Zeyen, E., Gallego-Castillo, C., & Victoria, M. (2024). Distributed photovoltaics provides key benefits for a highly renewable European energy system. Applied Energy, 360, 122721.

[8] Wang, L., Yuan, M., Zhang, F., Wang, X., Dai, L., & Zhao, F. (2019). Risk assessment of distribution networks integrating large-scale distributed photovoltaics. IEEE access, 7, 59653-59664.

[9] Fernández, G., Galan, N., Marquina, D., Martínez, D., Sanchez, A., López, P., ... & Rueda, J. (2020). Photovoltaic generation impact analysis in low voltage distribution grids. Energies, 13(17), 4347.

[10] Makinde, K. A., Akinyele, D. O., & Amole, A. O. (2021). Voltage rise problem in distribution networks with distributed generation: a review of technologies, impact and mitigation approaches. Indonesian Journal of Electrical Engineering and Informatics (IJEEI), 9(3), 575-600.

[11] M. Eltamaly, A., Sayed Mohamed, Y., M. El-Sayed, A. H., A. Mohamed, M., & Nasr A. Elghaffar, A. (2020). Power quality and reliability considerations of photovoltaic distributed generation. Technology and Economics of Smart Grids and Sustainable Energy, 5(1), 25.

[12] Li, Y., Sun, Y., Li, K., Zhuang, J., Liang, Y., & Pang, Y. (2021). Analysis and suppression of voltage violation and fluctuation with distributed photovoltaic integration. Symmetry, 13(10), 1894.

[13] Pei, C., Wang, Q., Zheng, Y., Li, G., Zheng, Z., & Hao, J. (2018, October). Research on voltage exceeding limits of active distribution network caused by distributed photovoltaic. In 2018 2nd IEEE Conference on Energy Internet and Energy System Integration (EI2) (pp. 1-4). IEEE.

[14] Ciocia, A., Boicea, V. A., Chicco, G., Di Leo, P., Mazza, A., Pons, E., ... & Hadj-Said, N. (2018). Voltage control in low-voltage grids using distributed photovoltaic converters and centralized devices. IEEE Transactions on Industry Applications, 55(1), 225-237.

[15] Ku, T. T., Lin, C. H., Chen, C. S., & Hsu, C. T. (2018). Coordination of transformer on-load tap changer and PV smart inverters for voltage control of distribution feeders. IEEE transactions on industry applications, 55(1), 256-264.

[16] Spertino, F., Ciocia, A., Mazza, A., Nobile, M., Russo, A., & Chicco, G. (2022). Voltage control in low voltage grids with independent operation of on-load tap changer and distributed photovoltaic inverters. Electric Power Systems Research, 211, 108187.

[17] Zhang, J., Wang, T., Chen, J., Liao, Z., & Shu, J. (2023). Cluster voltage control method for “Whole County” distributed photovoltaics based on improved differential evolution algorithm. Frontiers in energy, 17(6), 782-795.

[18] Ajayi, G. O., Dada, J. O., Osaloni, O. O., Adejumobi, B. S., Onibonoje, M. O., & Akinyele, W. S. (2025). Optimizing Distributed Generation Placement for Voltage Stability Using Genetic Algorithms Optimizing Distributed Generation Placement for Voltage Stability Using Genetic Algorithms. NIPES JSTR SPECIAL ISSUE, 7(2), 3083-3091.

[19] Wang, S., Lin, X., Chen, Z., Xu, Y., & Su, Q. (2024, November). Research on Distributed Photovoltaic Autonomous Optimization Control Strategy Under the Guidance of Voltage Optimization Principle. In 2024 IEEE 4th International Conference on Data Science and Computer Application (ICDSCA) (pp. 256-260). IEEE.

[20] Liu, H., Li, H., Li, J., & Shao, L. (2024). Distributed photovoltaic reactive power control strategy based on improved multiobjective particle swarm algorithm. Energy Science & Engineering, 12(11), 4904-4917.

[21] Kewen, L., Lei, Y., Qianyi, C., Xinhao, L., Shifeng, O., & Lyuzerui, Y. (2025). Voltage Regulation for PV-integrated Power Grid using Improved Multi-Objective Particle Swarm Optimization. Recent Advances in Electrical & Electronic Engineering, 18(8), 1335-1347.

[22] Santos, B. L., Barbosa, D., Barros, L. S., & Moreira, F. A. (2023). Photovoltaic Hosting Capacity Maximization of Low-Voltage Distribution Systems Based on Search of Optimal Power Factor for Interface Inverters Through Particle Swarm Optimization. Journal of Control, Automation and Electrical Systems, 34(6), 1260-1271.

[23] Ping, B., Zhang, X., Song, Q., Yu, Y., Wu, N., & Ji, X. (2020, November). Voltage control strategy for integrated medium and low voltage distribution network based on active-reactive power coordination optimization. In 2020 Chinese Automation Congress (CAC) (pp. 1187-1192). IEEE.

[24] Guan, X., Shao, D., Jiang, W., Shao, B., & Ma, Y. (2024, November). A SVC Voltage Regulation Control Strategy of Active Distribution Network Based on Improved Particle Swarm Algorithm. In 2024 IEEE 7th Student Conference on Electric Machines and Systems (SCEMS) (pp. 1-6). IEEE.

[25] Weng, H., Zhu, W., & Wu, J. (2025). Multi mode coordinated control algorithm for DC near-field photovoltaic based on adaptive mutation particle swarm optimization. Ain Shams Engineering Journal, 16(1), 103168.

[26] Liu, X., Zhao, P., Qu, H., Liu, N., Zhao, K., & Xiao, C. (2025). Optimal Placement and Sizing of Distributed PV-Storage in Distribution Networks Using Cluster-Based Partitioning. Processes, 13(6), 1765.